

## The Derivation of Carbon-Proton Internuclear Distances in Organic Natural Products from $^{13}\text{C}$ Relaxation Rates and Nuclear Overhauser Effects

Neri Niccolai and Claudio Rossi

Department of Chemistry, University of Siena, 53100 Siena, Italy

Paolo Mascagni and William A. Gibbons\*

Department of Pharmaceutical Chemistry, School of Pharmacy, University of London, London WC1N 1AX

Vittorio Brizzi

Institute of Pharmaceutical Chemistry, University of Siena, 53100 Siena, Italy

The precise definition of the hydrogen bonding patterns of natural product organic molecules and biopolymers in solution has hitherto been very difficult. It is demonstrated here that proton-carbon n.O.e. difference spectroscopy and carbon relaxation rates readily yield carbon assignments, the donor and acceptor groups of hydrogen bonds, and the *cis*- and *trans*- stereochemistry around C-O and C-N single bonds.

N.O.e. ratio methods and cross-relaxation rates gave proton-carbon distances that are in good agreement with the corresponding crystallographically derived distances.

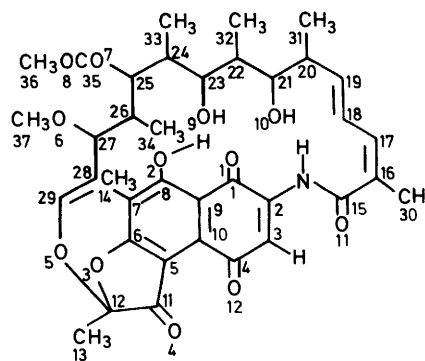
The use of proton relaxation rates<sup>1-4</sup> and  $^1\text{H}$ - $^1\text{H}$  nuclear Overhauser effects (n.O.e.s)<sup>5-8</sup> to determine molecular and biomolecular conformations is now widespread. It has been demonstrated that the n.O.e. ratio method,<sup>7</sup> cross-relaxation rates,<sup>2,3,8</sup> and time-dependent n.O.e.s<sup>5</sup> yield proton-proton distances, and that the last-named method yields conformational information. Conformational dynamics can also be elucidated from these parameters and from carbon relaxation rates.<sup>9,10</sup> Most recently, two dimensional n.O.e. methods have been introduced<sup>11,12</sup> but few quantitative results such as accurate distances have been obtained from these spectra.

One of the major remaining problems in studying solution conformation is the elucidation of the nature of each of the component moieties involved in intramolecular hydrogen bonds and of the proton-carbon and proton-nitrogen distances characteristic of each hydrogen bond in the molecule. A preliminary account of such an investigation for model compounds<sup>13,14</sup> and for the natural product rifamycin S<sup>15</sup> has appeared. Here we present a full account of our proton-carbon n.O.e. studies of rifamycin S. (Figure 1).

Rifamycin S was chosen for the following reasons: (i) its  $^1\text{H}$  and  $^{13}\text{C}$  n.m.r. spectra exhibit well-resolved chemical shifts<sup>16</sup> allowing effective selective proton irradiation and unequivocal assignments of observed  $^1\text{H}$ - $^{13}\text{C}$  n.O.e.s (Figures 2 and 3); (ii) rifamycin S, like other ansamycin antibiotics, is a molecule of considerable biological interest; (iii) the crystal structures of some of its derivatives has been determined,<sup>17</sup> permitting comparison with the solution conformation; and (iv) rifamycin S is very soluble in chloroform and the  $^{13}\text{C}$  n.m.r. sensitivity problems can be circumvented by the use of concentrated samples. Furthermore, the molecular shape and size of this molecule and the viscosity of this solvent should give rise to isotropic Brownian motions which are far outside the  $\omega_c\tau_c \gg 1$  limit.

### Results and Discussion

**Theory.**—N.O.e.s generated by broad band decoupling do not themselves yield any structural information.<sup>9,10</sup> Determinations of proton-carbon cross-relaxation rates from spin-lattice  $^{13}\text{C}$  relaxation rates,<sup>18</sup> selective n.O.e.s,<sup>19,20</sup> and 2 D n.O.e.s<sup>21</sup> for structural analyses have appeared, but the quantification of the observed effects to yield proton-carbon internuclear distances has not been reported.



Rifamycin S

**Figure 1.** The structure of rifamycin S with the atom numbering used in the present discussion. The aromatic and amidic moieties are shown in the conformations suggested by their proton-carbon cross-relaxation rates

Selective pre-saturation of a proton  $H_a$ , which interacts dipolarly through space with a  $^{13}\text{C}$  nucleus  $C_b$  at a distance  $r_{ab}$ , generates an n.O.e. given by:

$$\text{NOE}_{C_b}(H_a) = \gamma_H/\gamma_C [(W_2 - W_0)/R_{C_b}] \quad (1)$$

where

$$(\gamma_H/\gamma_C)(W_2 - W_0) = \sigma_{ab} = \left[ \frac{\hbar^2 \gamma_H^3 \gamma_C}{10 r_{ab}^6} \right] \left[ \frac{6\tau_c}{1 + (\omega_H + \omega_C)^2 \tau_c^2} - \frac{\tau_c}{1 + (\omega_H - \omega_C)^2 \tau_c^2} \right] \quad (2)$$

and  $R_{C_b}$  is the spin-lattice relaxation rate measured for  $C_b$  under broadband decoupling conditions. [For a definition of the quantities in equations (1) and (2) see ref. 5.]

Thus, by combining selective n.O.e. measurements and spin-lattice relaxation rates, information on single proton-carbon distances can be obtained from the calculated cross-relaxation rates ( $\sigma$ ).

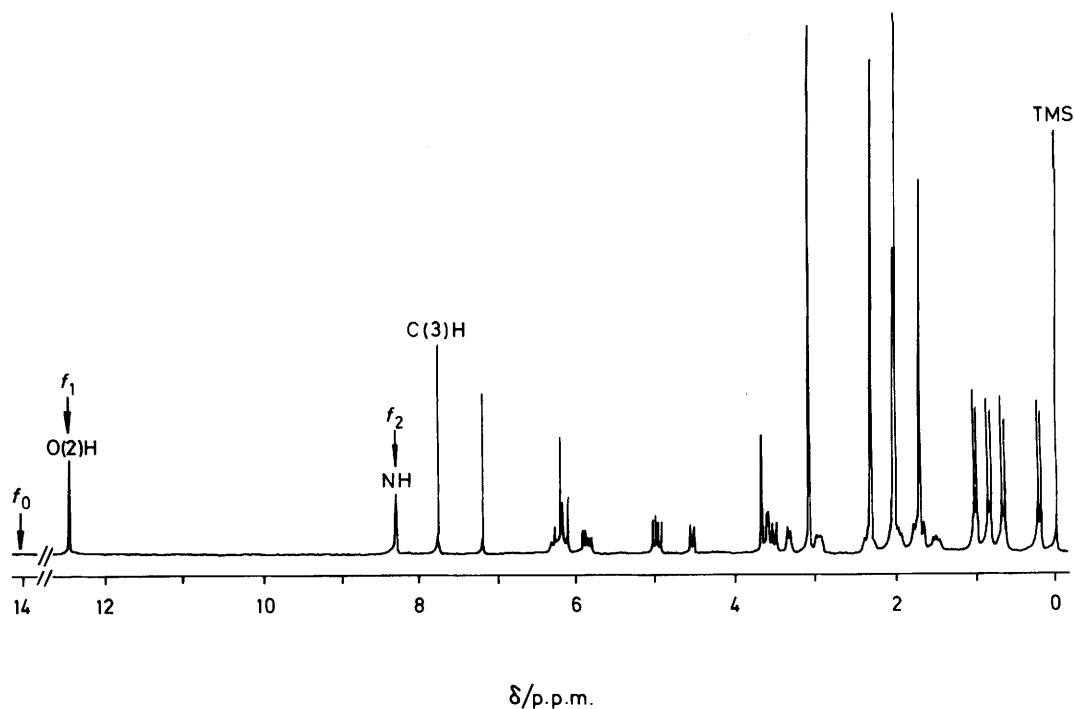


**Figure 2.** 200 MHz  $^1\text{H}$  N.m.r. spectrum of rifamycin S in  $\text{CDCl}_3$ . The arrows indicate the frequencies chosen for the low-power decoupler irradiations used for the selective proton-carbon Overhauser effect determination

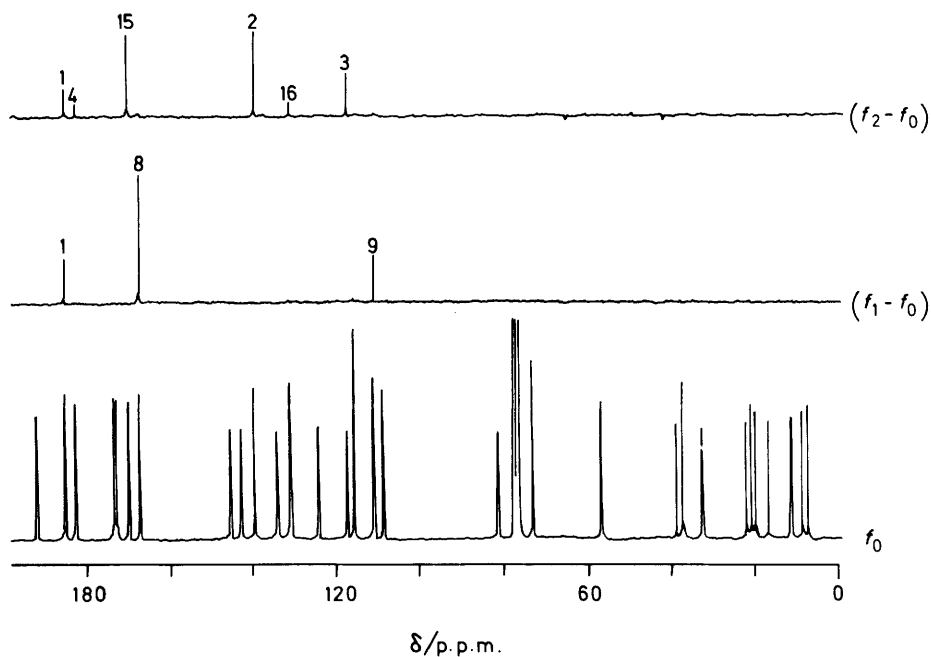


**Figure 3.**  $^{13}\text{C}$  N.m.r. spectrum of rifamycin S in  $\text{CDCl}_3$  obtained with the selective low-power decoupler positioned as  $f_0$  of Figure 2.  $(f_2 - f_0)$  and  $(f_1 - f_2)$  are difference spectra obtained by subtracting the  $f_0$  off-resonance spectrum with the other two recorded during selective decoupling at the  $f_1$  and  $f_2$  frequencies shown in Figure 2. In the n.o.e. difference spectra, the assignments of  $^{13}\text{C}$  resonances are shown

Provided cross-relaxation rates are calculated, two independent methods can be used to determine the proton-carbon internuclear distances.

*Method A.* When the saturation of  $\text{H}_a$  results in Overhauser effects on two or more carbon resonances, internuclear distances can be calculated from the following type of relationship:

$$\frac{\text{NOE}_{C_1}(\text{H}_a)R_{C_1}}{\text{NOE}_{C_2}(\text{H}_a)R_{C_2}} = \frac{r_{C_2\text{H}_a}^6}{r_{C_1\text{H}_a}^6} \quad (3)$$

To evaluate distances from equation (5), no prior knowledge of  $\tau_c$  is required, but one of the two distances, that does not depend on conformation or motion, is needed for calibration.

**Method B.** If both  $\tau_c$  and  $\sigma$  can be determined, an absolute calculation of distance is possible using the following equation.

$$r_{ab}^6 = \left[ \frac{\hbar^2 \gamma_H^3 \gamma_C}{10 \text{NOE}_{C_c}(\text{H}_a) R_{C_c}} \right] \left[ \frac{6\tau_c}{1 + (\omega_H + \omega_C)^2 \tau_c^2} - \frac{\tau_c}{1 + (\omega_H - \omega_C)^2 \tau_c^2} \right] \quad (4)$$

Which of these two methods is more useful depends on the particular system being investigated. In general, they should both be used on the same system, thus allowing a double check on the calculated  $r$  distances and the assumptions involved.

Complementary approaches to determine the internuclear distances involve the determination of the time dependence of the n.O.e.

**Relaxation Mechanisms.**—A complete study of the  $^{13}\text{C}$  spin-lattice relaxation rates of rifamycin S carbon resonances was carried out; the assignments and chemical shifts were consistent with previous reports. Furthermore, in order to gain information on relaxation mechanisms and molecular dynamics a quantitative analysis of the observed Overhauser effects, obtained after continuous broad band proton decoupling, was carried out. The interpretation of the data, shown in Table 1, was used as a starting point for a further structural investigation, as carbon nuclei involved in such a study must relax, partially at least, through  $^1\text{H}$ - $^{13}\text{C}$  dipolar interactions, modulated by molecular motions outside the  $(\omega_H + \omega_C)\tau_c > 1$  limit.

In Table 1, the carbon nuclei of rifamycin S have been divided into three groups, depending on the number of attached protons. Each member of these groups exhibited relaxation rates typical of the group. As expected, all protonated carbons exhibited similar and fast  $R$  values, while quaternary carbons relaxed very slowly. Intermediate relaxation behaviour was observed for methyl carbon nuclei.

Before the  $^{13}\text{C}$  relaxation rates were analysed in terms of molecular motions and proton environments, the measured non-selective n.O.e.s and broad band n.O.e.s [NOE(BB)] were compared with those theoretically expected for  $^{13}\text{C}$  atoms totally relaxing through  $^1\text{H}$ - $^{13}\text{C}$  dipolar interactions. The fast reorientation of the methyl carbon should satisfy the  $(\omega_H + \omega_C)\tau_c \ll 1$  limit; hence, for these we would expect the maximum n.O.e. NOE<sub>0</sub>, of 1.988. Thus, the fractional effectiveness of the dipolar relaxation of the methyl carbons is given by NOE/1.988. The uniformity of the values shown in Table 1 (column 4) confirms that the methyl carbons relax essentially through dipolar interactions with the bound proton nuclei.

The analogous methine carbons attached directly to the skeleton of rifamycin S appear to relax slightly outside the extreme narrowing condition,  $(\omega_H + \omega_C)\tau_c \ll 1$ . A maximum theoretical n.O.e. of 1.90 gave, in general, the expected NOE(BB)/1.90 ratios of 1. This maximum n.O.e. is consistent with  $\tau_c = 2.0 \times 10^{-10}$  s, and can be used to determine  $^{13}\text{C}$  relaxation rates of CH's similar to those in Table 1. The assumption is made that the methine carbons, like the methyls, relax predominantly by a dipolar mechanism.

Similar correlation times should modulate the methine and quaternary carbons of rifamycin S owing to the isotropic reorientation of this molecule. The NOE(BB)/1.90 ratios of quaternary carbons thus indicate that their poor proton environment possibly results in some contributions from non-dipolar relaxation.

**Proton-Carbon Internuclear Distances.**—As shown in Figure 3 the selective saturation of the O(2)H and the amide NH protons generated a limited number of carbon n.O.e.s of

**Table 1.** Observed and calculated relaxation parameters and n.O.e.s for rifamycin S in  $\text{CDCl}_3$

$\text{C}(n)\text{H}_3$	$\delta/\text{p.p.m.}^a$	$R^d$	$[\text{NOE}(\text{BB})/1.988]^e$	$[\text{R}^{\text{DD}}/3]^f$
13	22.00	3.57	1.0	1.19
14	7.31	1.14	0.9	0.34
30	19.89	1.35	1.0	0.45
31	16.69	3.57	1.0	1.19
32	11.48	1.95	0.9	0.58
33	8.63	1.59	1.2	0.53
34	11.15	1.93	0.9	0.64
36	20.86	1.23	1.0	0.41
37	56.59	1.11	0.9	0.33

$\text{C}(n)\text{H}$	$\delta/\text{p.p.m.}$	$R$	$[\text{NOE}(\text{BB})/1.90]^e$	$[\text{R}^{\text{DD}}]^f$
3	118.88	5.88	1.1	5.88
17	133.66	5.88	0.8	4.70
18	123.91	5.26	1.0	5.26
19	141.98	5.00	0.9	4.50
20	38.82	5.26	1.0	5.26
21	73.24	5.26	1.0	5.26
22	32.56	5.88	1.1	5.88
23	<i>b</i>	<i>b</i>	<i>b</i>	<i>b</i>
24	37.16	5.55	1.1	5.55
25	73.24	5.26	1.0	5.26
26	37.16	5.55	1.1	5.55
27	81.36	5.26	1.3	5.26
28	115.55	4.54	0.8	3.63
29	144.60	4.76	1.0	4.76

$\text{C}(n)\text{H}$	$\delta/\text{p.p.m.}$	$R$	$[\text{NOE}(\text{BB})/1.90]^e$	$[\text{R}^{\text{DD}}]^f$
1	184.57	0.34	0.4	0.13
2	138.92	0.50	0.6	0.30
4	181.88	0.31	0.3	0.09
5	110.61	0.16	0.2	0.03
6	172.33	0.43	0.2	0.08
7	114.31	0.32	0.2	0.06
8	166.59	0.23	0.6	0.14
9	110.51	0.23	0.3	0.07
10	130.66	0.21	0.2	0.04
11	191.46	0.21	0.3	0.06
12	108.21	0.22	1.1	0.22
15	169.31	0.40	0.7	0.28
16	130.38	0.37	0.7	0.28
35	172.83	0.45	0.6	0.27

<sup>a</sup> From internal  $\text{Me}_4\text{Si}$ . <sup>b</sup> C-23 overlaps with  $\text{CDCl}_3$  carbon resonances. <sup>c</sup> The  $\tau_c$  value of  $2.1 \times 10^{-10}$  s is different from that used for methyl groups but was needed to fit the methine data of column 4. <sup>d</sup>  $R$  and NOE(BB) values were experimentally measured. <sup>e</sup> NOE(BB)/1.988 etc. in column 4 represent the fractional effectiveness of the dipolar relaxation mechanisms. <sup>f</sup>  $\text{R}^{\text{DD}}/\text{no. of attached protons}$  is the relaxation contribution which is the product of columns 3 and 4.

differing magnitude. A qualitative inspection of these revealed some anomalies when NH was irradiated. For example, simultaneous detection of n.O.e.s on the C-1, C-3, and C-4 peaks is not consistent with the molecular structure. Decoupler spill-over effects were, therefore, investigated by the frequency dependence study shown in Figure 4. The n.O.e. data in Figure 4 permitted discrimination between real n.O.e.s and those generated by the decoupler spill-over. In fact, when the decoupler was positioned on-resonance on the NH proton at 8.35 p.p.m., maximum n.O.e.s were found at the C-1, C-2, C-15, and C-16 nuclei while, on shifting the decoupler upfield, the n.O.e.s measured for the C-3 and C-4 peaks increased. As the 3-H proton resonates upfield from the NH proton, the decoupler spill-over was considered to be responsible for the last two

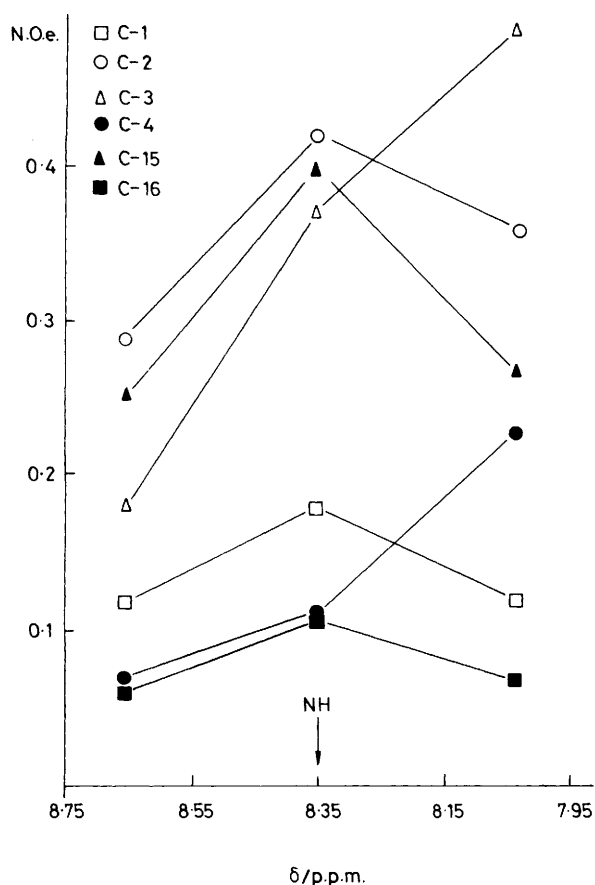


Figure 4. Variation of the n.O.e. effects on the C atoms of rifamycin S as a function of the proton irradiation frequency

n.O.e.s. The direct  $^{13}\text{C}_3\text{-}^1\text{H}$  scalar coupling constant,  $^1J_{\text{C}_3\text{H}_4}$ , 180 Hz, gave two satellite proton resonances at 7.35 and 8.25 p.p.m., while the small geminal coupling constant  $^2J_{\text{C}_4\text{H}_3}$  for the  $^{13}\text{C}(4)^{13}\text{C}(3)^1\text{H}$  fragment gave satellite peaks close to the proton resonance at 7.80 p.p.m. Accordingly, the on-resonance decoupler position of a given proton is  $J$  modulated by the  $^{13}\text{C}$  nucleus, and this effect must be taken into account in the quantitative determination of heteronuclear cross-relaxation rates, as the dipolar interactions occur at the frequency of these proton satellite resonances. This explains the difference in the frequency dependence of the n.O.e.s measured for C-3 and C-4.

**Method A.** The geminal distances  $^{13}\text{C}(2)\text{-NH}$  and  $^{13}\text{C}(8)\text{-O}(2)\text{H}$  are both equal to 2.00 Å and to a first-order approximation are independent of conformation and motion. The n.O.e.s obtained by selective irradiation of the  $^{13}\text{C}(2)\text{-NH}$  were used to calculate the distances  $r_X$  and  $r_M$  entries in Table 2 obtained by crystallography, as did those ( $r_A$ ) calculated from the  $^{13}\text{C}(8)\text{-O}(2)\text{H}$  calibration distances.

Although the conformation of rifamycin had been previously determined by crystallography these results suggest that method A can be used to delineate accurately and quantitatively the conformation in natural products of unknown structures.

The success of these results also suggests that, at least for rifamycin S, a similar correlation time modulates the relaxation of the relevant  $^1\text{H}\text{-}^{13}\text{C}$  vectors. Hence, if we evaluate this correlation time method B should be applicable to distance measurement.

**Method B.** For this method the correlation time and the cross-relaxation rates between the relevant protons and carbons are required. The value of  $\tau_c$  was available from three sources. The two calibration distances of the previous paragraphs and their measured  $\sigma$  values ( $\sigma_{\text{NH}(2)} = 0.210 \text{ s}^{-1}$ ) gave  $\tau_c = 2.1 \times 10^{-10} \text{ s}$ . This is the same  $\tau_c$  value as was needed to fit the experimental and calculated ratios of the broad band continuous methine n.O.e.s to the maximum n.O.e.s in Table 1 on the assumption that methines relax by dipolar mechanisms.

This value of  $\tau_c$  when used with the various  $^1\text{H}\text{-}^{13}\text{C}$  n.O.e.s gave the distances  $r_B$  in Table 2. The latter values agreed with the  $r_A$  values and the crystallographic values.

These proton-carbon distances obtained from  $^{13}\text{C}$  relaxation parameters can therefore be used with confidence for a conformational analysis of rifamycin S. The experimentally derived  $r_{\text{C}(1)\text{NH}} = 2.45 \text{ Å}$  showed that, under our experimental conditions, C-3 and the amide proton are predominantly in the *trans* conformation. In fact, in the presence of the two isomers under fast exchange conditions, the measured  $\sigma$  is an averaged value:

$$\langle \sigma \rangle = P_{\text{cis}}\sigma_{\text{cis}} + P_{\text{trans}}\sigma_{\text{trans}} \quad (5)$$

where  $P_{\text{cis}}$  and  $P_{\text{trans}}$  are the fractional populations of the *cis*- and *trans*-isomers. Therefore, the effective internuclear distance is given by:

$$\langle 1/r^6 \rangle = P_{\text{cis}}(1/r_{\text{cis}}^6) + P_{\text{trans}}(1/r_{\text{trans}}^6) \quad (6)$$

Thus, owing to the intrinsic  $r_{\text{cis}}$  and  $r_{\text{trans}}$  values (see Table 2), the calculated  $r_{\text{C}(1)\text{NH}}$  can be consistent only with a very small

Table 2. A comparison of proton-carbon distances obtained by computer modelling ( $r_M$ ) and crystallography ( $r_X$ ) with those determined from  $^1\text{H}\text{-}^{13}\text{C}$  n.O.e.s and  $^{13}\text{C}$   $\tau_1$  values using methods A ( $r_A$ ) and B ( $r_B$ )

Carbon	C(n)-NH				C(n)-O(2)H						
	$r_X^a$	<i>cis</i> $r_M^b$	<i>trans</i> $r_M^b$	$\tau_1(\text{HC})_M^c$	$r_A^c$	$r_B^d$	$r_X^a$	$r_M^b$	$\tau_1(\text{HC})_M^c$	$r_A^e$	$r_B^d$
1	2.453	2.670	3.367		2.4 <sub>5</sub>	2.4 <sub>5</sub>	2.383	2.352		2.1 <sub>9</sub>	2.2 <sub>0</sub>
2	1.911	2.141	2.141	0.061					0.117		
3	3.131	3.367	2.670	0.210							
7							3.266	3.199		3.0 <sub>5</sub>	3.0 <sub>6</sub>
8							2.023	1.938	0.016		2.0 <sub>0</sub>
9							2.541	2.463	0.204	2.3 <sub>4</sub>	2.3 <sub>5</sub>
15	1.934	2.160			2.0 <sub>9</sub>	2.0 <sub>9</sub>			0.078		
16	2.471	2.757			2.6 <sub>7</sub>	2.6 <sub>7</sub>					
17				0.037							

<sup>a</sup> Proton-carbon distance calculated from X-ray data in ref. 13. <sup>b</sup> Proton-carbon distance derived from computer modelling. <sup>c</sup>  $r_A$  Values were evaluated using equation (5) and  $r_{\text{C}(2)\text{NH}} = r_{\text{C}(8)\text{HO}(2)} = 2.00 \text{ Å}$ . <sup>d</sup>  $r_B$  Values obtained from equation (6),  $\sigma$  values and  $\tau_c = 2.1 \times 10^{-10} \text{ s.r.v.}$  <sup>e</sup> Cross-relaxation rates ( $T_1 \text{ s}^{-1}$ ) are affected by the errors on n.O.e. and  $R$  values

fractional population of the *cis*-isomer,  $P_{cis}$ . It follows that the n.O.e. observed at C-3 upon proton irradiation at 8.35 p.p.m. must be entirely due to the decoupler spill-over. The presence of the intramolecular hydrogen bonding pattern between the O(2)H proton and the C(1)=O carbonyl is unambiguously delineated from the  $R_{C(1)O(2)H}$  value of 2.20 Å. As a corollary of the present study, the assignment of  $^{13}C$  peaks and the sequencing of the C(1)NHC(15)OC(16) moiety of rifamycin S was confirmed.

### Experimental

Rifamycin S (Figure 1) was purified from the commercially available drug and dissolved in deuteriochloroform to yield a 0.5M-solution. A Varian XL-200 n.m.r. spectrometer was used for recording the  $^1H$  and  $^{13}C$  n.m.r. spectra (see Figures 2 and 3). The partially relaxed  $^{13}C$  n.m.r. spectra were obtained with the standard inversion recovery  $(180 - \tau - 90^\circ - T)_n$  pulse sequence. The calculation of  $R$  values was performed by computer fitting of the  $M_z$  value versus relaxation curves. A 5% experimental error was estimated for the  $R$  values reported in Table 1. A low-power selective presaturating proton decoupler pulse of 10-s duration generated the  $^1H-^{13}C$  Overhauser effects, as shown in Figure 2; a  $90^\circ$  pulse was used for detection. An experimental error of 10% was estimated for all measured n.O.e.s. The high power decoupler was used during this observing pulse and for the 0.6 s required for the acquisition of the free induction decay. A 40-s delay was used to allow complete relaxation of the perturbed spin systems. Broad band non-selective  $^1H-^{13}C$  n.O.e.s were measured from fully relaxed spectra obtained under continuous and gated proton decoupling, with a 40-s delay between each  $90^\circ$  pulse. In all the experiments the temperature of the probe was  $25^\circ C \pm 1^\circ C$ .

### References

- 1 I. D. Campbell and R. H. Freeman, *J. Magn. Reson.*, 1973, **11**, 143.
- 2 R. H. Freeman, D. W. Hill, B. L. Tomlinson, and L. D. Hall, *J. Am. Phys.*, 1974, **61**, 4466.

- 3 N. Niccolai, H. K. Schnoes, and W. A. Gibbons, *J. Am. Chem. Soc.*, 1980, **100**, 1513.
- 4 N. Niccolai, M. P. Miles, S. P. Hehir, and W. A. Gibbons, *J. Am. Chem. Soc.*, 1980, **100**, 1412.
- 5 J. H. Noggle and R. E. Schirmer, 'The Nuclear Overhauser Effect,' Academic Press, New York, 1971.
- 6 W. A. Gibbons, D. Crepau, J. Delayre, J. J. Dunand, G. Hajdukovic, and H. R. Wyssbrod in 'Peptides: Chemistry, Structure and Biology, Proceedings of the Fourth American Peptide Symposium,' eds. R. Walter and J. Meinhofer, Ann Arbor Science Publishers, Inc. Ann Arbor, 1975, p. 125.
- 7 C. R. Jones, C. T. Sikakana, S. Hehir, M. R. Kuo, and W. A. Gibbons, *Biophys J.*, 1978, **24**, 815.
- 8 C. R. Jones, C. T. Sikakana, M. C. Kuo, and W. A. Gibbons, *J. Am. Chem. Soc.*, 1978, **100**, 5960.
- 9 D. Doddrell, U. Glushko, and A. Allerhand, *J. Chem. Phys.*, 1972, **56**, 3683.
- 10 K. F. Kuhlman, D. M. Grant, and R. Harris, *J. Chem. Phys.*, 1970, **52**, 3439.
- 11 A. Kumar, R. R. Ernst, and K. Wuthrich, *Biochem. Biophys. Res. Commun.*, 1980, **95**, 1.
- 12 S. Macura and R. R. Ernst, *Mol. Phys.*, 1980, **41**, 95.
- 13 J. J. Ford, W. A. Gibbons, and N. Niccolai, *J. Magn. Reson.*, 1982, **47**, 522.
- 14 N. Niccolai, L. Pogliani, E. Tiezzi, and C. Rossi, *Nuovo Cimento*, 1984, in the press.
- 15 N. Niccolai, C. Rossi, U. Brizzi, and W. A. Gibbons, *J. Am. Chem. Soc.*, 1984, in the press.
- 16 U. Brizzi, M. Brufani, L. Cellai, and A. L. Segre, *J. Antibiot.*, 1983, **36**, 516.
- 17 M. Brufani, L. Cellai, S. Cerrini, W. Fedeli, and A. Vaciago, *Mol. Pharmacol.*, 1978, **14**, 693.
- 18 M. J. Shapiro and A. D. Khale, *Org. Magn. Reson.*, 1979, **12**, 235.
- 19 J. Uzawa and S. Takeuchi, *Org. Magn. Reson.*, 1978, **11**, 502.
- 20 M. S. Aldersley, F. M. Dean, and B. E. Mann, *J. Chem. Soc., Chem. Commun.*, 1983, 107.
- 21 P. L. Rinaldi, *J. Am. Chem. Soc.*, 1983, **105**, 5167.

Received 3rd April 1984; Paper 4/548